

Intracortical circuits of pyramidal neurons reflect their long-range axonal targets

Solange P. Brown¹ & Shaul Hestrin¹

Cortical columns generate separate streams of information that are distributed to numerous cortical and subcortical brain regions¹. We asked whether local intracortical circuits reflect these different processing streams by testing whether the intracortical connectivity among pyramidal neurons reflects their long-range axonal targets. We recorded simultaneously from up to four retrogradely labelled pyramidal neurons that projected to the superior colliculus, the contralateral striatum or the contralateral cortex to assess their synaptic connectivity. Here we show that the probability of synaptic connection depends on the functional identities of both the presynaptic and postsynaptic neurons. We first found that the frequency of monosynaptic connections among corticostriatal pyramidal neurons is significantly higher than among corticocortical or corticotectal pyramidal neurons. We then show that the probability of feed-forward connections from corticocortical neurons to corticotectal neurons is approximately three- to four-fold higher than the probability of monosynaptic connections among corticocortical or corticotectal cells. Moreover, we found that the average axodendritic overlap of the presynaptic and postsynaptic pyramidal neurons could not fully explain the differences in connection probability that we observed. The selective synaptic interactions we describe demonstrate that the organization of local networks of pyramidal cells reflects the long-range targets of both the presynaptic and postsynaptic neurons.

The long-range axonal projections of cortical pyramidal neurons target unique sets of cortical and subcortical brain regions and define different functional classes of pyramidal neuron¹. In addition, each pyramidal neuron elaborates extensive intracortical axon collaterals that generate the majority of excitatory input in neighbouring cortical neurons^{2–4}. Recent work has shown that the probability of connection among pyramidal neurons is not homogeneous^{5–11}. However, whether local synaptic interactions reflect the long-range axonal projections of both the presynaptic and the postsynaptic partner is not known.

Non-overlapping populations of pyramidal neurons projecting to different brain regions are intermingled within layer 5 (L5), the main output layer of the cortex¹. We first compared the homotypic connectivity among L5 pyramidal neurons projecting to different brain regions. To address this question, we injected fluorescent latex microspheres into the ipsilateral superior colliculus to label corticotectal neurons, the contralateral striatum to label corticostriatal neurons, or the contralateral visual cortex to label corticocortical neurons. We next recorded in whole cell configuration from fluorescently labelled neurons and determined that the intrinsic physiological properties of corticotectal, corticostriatal and corticocortical pyramidal neurons were significantly different (Supplementary Fig. 1, Supplementary Table 1), as expected for three distinct classes of pyramidal neuron^{12–14}.

To assay the synaptic connectivity among pyramidal neurons projecting to the same long-range target, we recorded simultaneously

from multiple fluorescently labelled neurons using whole-cell patch clamp techniques. Action potentials were generated with brief current injections in each neuron in turn while the synaptic responses in the other neurons were recorded. In synaptically connected cells, these presynaptic action potentials elicited monosynaptic unitary excitatory postsynaptic potentials (EPSPs) in the postsynaptic partner. Monosynaptic connections were identified between neurons for all three cell types (Fig. 1a–c). The synaptic properties, including the mean amplitudes and the paired-pulse ratio, were similar among the three types of connection (Supplementary Table 2).

Although the properties of the synaptic responses were similar, the rate of monosynaptic connections among corticostriatal neurons was

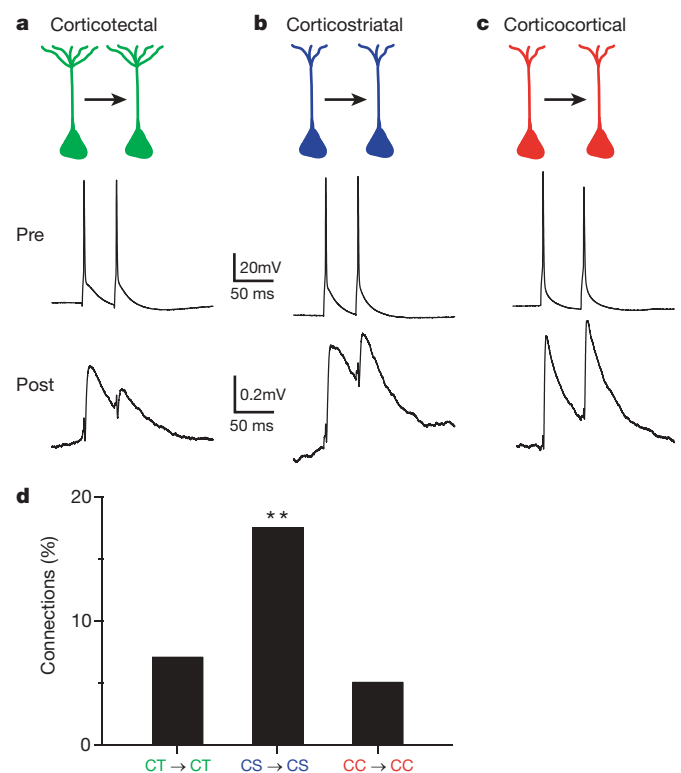


Figure 1 | Different frequencies of monosynaptic connections between corticotectal, corticostriatal or corticocortical neurons. **a, b, c,** Presynaptic action potentials elicit a synaptic response in a postsynaptic cell during simultaneous recordings from two monosynaptically connected corticotectal neurons (**a**), corticostriatal neurons (**b**) and corticocortical neurons (**c**). **d,** The frequency of identified monosynaptic connections among connections tested is shown for corticotectal (CT) connections, corticostriatal (CS) connections and corticocortical (CC) connections. ** $P < 0.05$.

¹Department of Comparative Medicine, Stanford University School of Medicine, 300 Pasteur Drive, Edwards Building, R314, Stanford, California 94305-5342, USA.

significantly higher than the rate among corticotectal neurons or among corticocortical neurons. Eighteen per cent of corticostriatal-to-corticostriatal potential connections tested were monosynaptically connected (seven of 40 tested connections), a considerably higher connectivity than previously reported for L5 pyramidal neurons^{6,10,11,15,16}. By contrast, only 7% of potential corticotectal-to-corticotectal connections (16 of 225 tested connections) and 5% of potential corticocortical-to-corticocortical connections (6 of 118 tested connections) were monosynaptically connected ($P = 0.034$, Pearson's chi-squared test; Fig. 1d). Our results indicate that specific functional classes of pyramidal neuron can form highly interconnected networks embedded within the local circuitry of the cortex.

Several connectivity schemes could underlie the observed differences in the probability of connection among these cell types. First, the corticotectal and corticocortical cells we studied were located in the visual cortex whereas the corticostriatal cells were located in the sensorimotor cortex, raising the possibility of a regional effect on cortical connectivity. Second, each presynaptic cell type could connect to its neighbours with a characteristic frequency. Corticostriatal neurons may simply connect to all their targets with a higher probability than corticotectal or corticocortical neurons. This interpretation is consistent with recent work showing that pyramidal neurons with different long-range projections have different probabilities of forming connections with neighbouring neurons^{10,11,17}, suggesting that, rather than reflecting axonal target selectivity *per se*, the probability of connection is a global property specific to each pyramidal cell type. Third, cortical circuits may reflect the functional identity of the presynaptic and postsynaptic cell types. In this case, the intracortical connectivity among pyramidal neurons may reflect the long-range axonal projections of both the presynaptic and postsynaptic pyramidal neurons. Whether pyramidal neurons can synapse differentially onto neighbouring pyramidal neurons of different functional classes is not known.

To differentiate among these possibilities, we targeted quadruplets composed of pyramidal neurons with two different long-range projections for electrophysiological recordings. This configuration allowed us to simultaneously compare the connectivity rates of two types of pyramidal neuron with two different postsynaptic targets. If the brain region or the functional identity of the presynaptic neuron dictates its connectivity with neighbouring pyramidal neurons, we expect that a pyramidal neuron's probabilities of connection with the two different postsynaptic targets are the same. However, if the probability of connection differs for the different types of connection, then intracortical connectivity depends on the functional identity of both the presynaptic neuron and the postsynaptic neuron.

We injected red fluorescent microspheres into the contralateral visual cortex and green fluorescent microspheres into the ipsilateral superior colliculus to label both corticocortical and corticotectal neurons in the same animal. We then recorded simultaneously from these classes of pyramidal neuron intermingled in L5 of the visual cortex, and directly compared the probability of connection for four types of connections: corticocortical to corticocortical, corticocortical to corticotectal, corticotectal to corticotectal, and corticotectal to corticocortical (Fig. 2a). We found that the probability of identifying corticotectal-to-corticocortical connections is 5% (4 of 86 connections tested), similar to the 7% probability of identifying a corticotectal-to-corticotectal connection ($P = 0.43$, Pearson's chi-squared test), indicating that corticotectal cells do not connect to corticocortical pyramidal neurons in preference to corticotectal pyramidal neurons. However, the probability of identifying a corticocortical-to-corticotectal connection is 19% (16 of 86 connections tested), whereas the probability of identifying a corticocortical-to-corticocortical connection is only 5% ($P = 0.002$, Pearson's chi-squared test; Fig. 2b), indicating that corticocortical pyramidal neurons preferentially target neighbouring corticotectal neurons.

Our results indicate that the probability of identifying connections between L5 pyramidal neurons in visual cortex is not universally low.

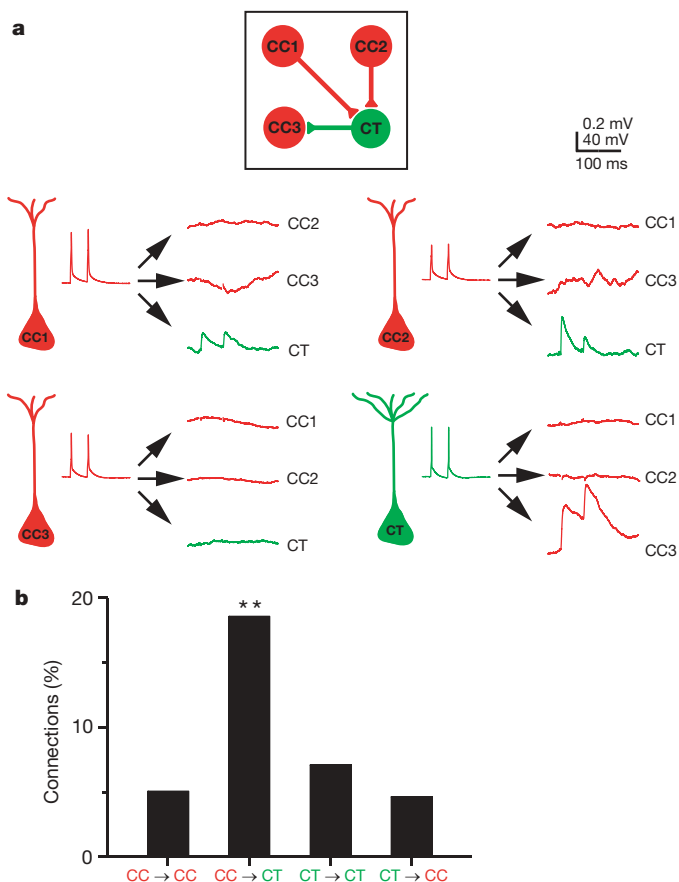


Figure 2 | The probability of connection depends on the identities of the presynaptic and the postsynaptic pyramidal cell types. **a**, An example of a quadruple recording. Three corticocortical neurons (CC1, CC2, CC3; red) and one corticotectal neuron (green) were recorded simultaneously and the 12 possible synaptic connections were tested. The corticocortical neurons CC1 and CC2 synapsed onto the neighbouring corticotectal neuron. The corticotectal neuron in turn synapsed onto the corticocortical neuron CC3. Scale bars: 40 mV for presynaptic action potentials, 0.2 mV for postsynaptic responses. **b**, The frequency of synaptic connections identified among the tested connections is shown for the four possible types of connection among corticocortical and corticotectal neurons. ** $P < 0.01$.

The probability of identifying corticocortical-to-corticotectal connections was as high as the probability of identifying corticostriatal-to-corticostriatal connections in the sensorimotor cortex. Our results further indicate that the connectivity among pyramidal neurons is not simply a global characteristic of the presynaptic or the postsynaptic neuron. A corticocortical axon is almost four times more likely to form a functional synapse with a local corticotectal pyramidal neuron than with a corticocortical pyramidal neuron, indicating that local intracortical circuits reflect the functional identity of the postsynaptic pyramidal neuron. Moreover, the probability of identifying a monosynaptic connection is 19% for corticocortical-to-corticotectal combinations but only 7% for corticotectal-to-corticotectal combinations, indicating that the long-range target of the presynaptic cell is also important. Combined, our results suggest that it is the interplay between the functional identities of the presynaptic and the postsynaptic pyramidal neurons that determines the pattern of local microcircuits in the cortex.

Several authors have suggested that pyramidal neurons synapse probabilistically onto neighbouring neurons, and that their connectivity is a function of the average spatial overlap of their dendritic and axonal processes^{4,18–21}. If this is the case, the connectivity rates that we measured may simply reflect different average spatial overlaps for the five connections we tested rather than any local selection among different functional types of pyramidal neuron. To evaluate

this possibility, we asked whether the frequencies of monosynaptic connections we measured could be explained by differences in the distribution of the axonal and dendritic processes for these cell types. To address this question, we first reconstructed the three-dimensional morphology of L5 pyramidal neurons of each type filled with biocytin during our physiological recordings. The reconstructions of the dendritic and axonal arbors are shown (in blue and red, respectively) in Fig. 3a–c. For each of the three cell types, the morphology of the L5 reconstructed neurons was similar^{11,12,22–24}, indicating that the intracortical morphology of each functional class was consistent. However, the distribution of the dendritic and axonal processes among the three cell types was clearly different (Supplementary Figs 2, 3, 4).

Next we asked whether these morphological differences could account for the differences in connectivity that we measured physiologically. To estimate the axodendritic overlap, we quantified the average local density of the dendritic and axonal processes for each cell by generating length density maps from the three-dimensional reconstructions for each type of process²⁵. We then calculated the product of the axonal length density map and the dendritic length density map for each combination of neurons that we studied electrophysiologically. Figure 3d shows the results for neurons separated by 50 μm , the average distance between neurons in our physiological data set (see Methods Summary). Separating neurons from 0 to 200 μm , the largest distance between neurons in our data set, produced similar results. These axodendritic overlaps estimate the potential numbers of synapses formed between each combination of cell types studied.

To determine whether the differences in axodendritic overlap could account for the functional connectivity that we measured, we next integrated the maps of axodendritic overlap to obtain the overall axodendritic overlap for each type of synaptic connection. The probability of connection and the axodendritic overlap for each of the cell combinations tested are plotted in Fig. 3e. If a doubling in axodendritic

overlap results in a doubling in the probability of connection, then the ratio of the axodendritic overlaps for two types of cell pair should be equal to the ratio of their probabilities of connection. However, the ratio of connection probabilities for corticocortical-to-corticotectal connections and corticocortical-to-corticocortical connections, for example, was 3.7, whereas the ratio of axodendritic overlaps was 1.6. The resulting ratio of these two numbers was significantly greater than one ($P = 0.03$). Previous work has shown that synapses among neighbouring L5 pyramidal neurons are largely located on the proximal dendrites^{10,11,15,26}. Restricting our analyses to the perisomatic dendrites produced similar results ($P = 0.02$). Taken together, our data preclude a straightforward linear relationship between the average axodendritic overlap and the probability of connection, and suggest that the average local density of axons and dendrites alone cannot explain the differences in the probability of connection.

Previous experiments have suggested that pyramidal neurons within L5 form a sparsely connected network, with probabilities of connection ranging from 1% to 12% (refs 6, 10, 11, 15, 16). Here we show that the probability of identifying monosynaptic connections among corticostriatal pyramidal neurons and feed-forward connections from corticocortical to corticotectal pyramidal neurons is approximately 20% per connection tested (equivalent to ~30–40% per pair tested). The excitatory monosynaptic connections among corticostriatal pyramidal neurons we describe could amplify the activation of interconnected ensembles of corticostriatal neurons, and the resulting coherent activity could depolarize functionally related striatal neurons, consistent with the hypothesis that the activity of many converging corticostriatal axons is required to depolarize postsynaptic striatal neurons^{27,28}. We show that, although corticocortical neurons are monosynaptically interconnected at low rates, as are corticotectal neurons, the local intracortical axons of corticocortical cells target corticotectal neurons with high probability. Interestingly, *in vivo* experiments showed that corticotectal cells were preferentially activated by callosal stimulation and suggested that

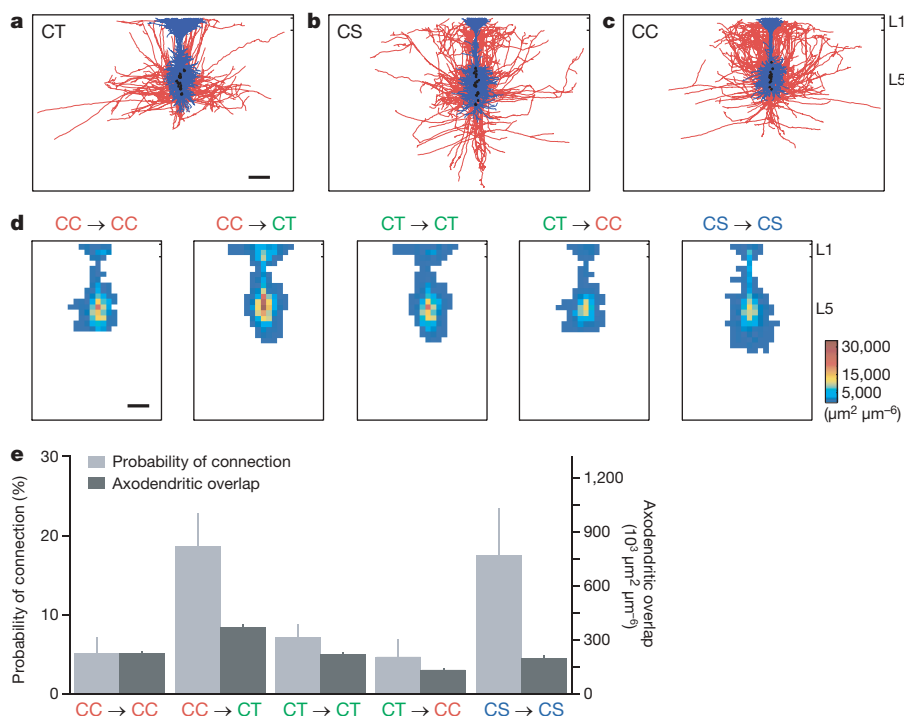


Figure 3 | The average axonal and dendritic architecture alone cannot explain differences in the connection probability. **a, b, c,** The morphology of 15 corticotectal (**a**), corticostriatal (**b**) and corticocortical neurons (**c**). Blue, dendrites; red, axons; black, somas. **d,** The dendritic and axonal length density maps were used to estimate the spatial overlap of the neuronal processes for the five types of connection tested physiologically. We display

the resulting maps of axodendritic overlap (colour scale), generated from cells aligned relative to the pial margin and shifted 50 μm relative to each other. Scale bars, 200 μm . **e,** The probability of physiological connection and the average axodendritic overlap are plotted for each type of connection tested.

feed-forward corticocortical input is important in generating the receptive field properties of corticotectal neurons^{29,30}. Our results indicate that the probability of connection among specific functional classes of pyramidal neurons can be quite high, and suggest that highly interconnected functional subnetworks are embedded within the local circuitry of L5.

How local cortical circuits generate the cortex's output remains an open question. Previous work has shown that the connectivity between two pyramidal neurons influences the synaptic input they receive, demonstrating the existence of interconnected subnetworks within the neocortex^{6,8,9}. We demonstrate that connections among pyramidal neurons reflect the long-range outputs of both the pre-synaptic and postsynaptic pyramidal neurons. Our results suggest an approach for understanding the function of specialized subnetworks embedded within cortical circuits. Unravelling the local circuits of pyramidal neurons whose long-range targets are known will allow us to understand how the different cortical outputs are generated within the cortical microcircuit. Given the diversity in the distant targets of pyramidal neurons, our findings suggest the existence of multiple networks of pyramidal neurons whose local intracortical connections subserve the specific roles played by their long-range axons.

METHODS SUMMARY

Mice (P14 to P17) were anaesthetized and fluorescently labelled latex microspheres (RetroBeads, Lumafluor) were injected into the ipsilateral superior colliculus, the contralateral striatum and the contralateral cortex to retrogradely label cortical neurons projecting to each target. One or more days later, parasagittal cortical slices were sectioned. Neurons labelled with fluorescent beads were targeted for simultaneous whole-cell patch clamp recordings and their synaptic connectivity was assessed (see Methods). The morphology of the recorded neurons was revealed with biocytin using standard techniques and was reconstructed in three dimensions. To estimate the spatial overlap of the axonal and dendritic processes of the presynaptic and postsynaptic cells, we determined the axonal and dendritic length density maps of each cell. The axonal length density map of each cell of the appropriate presynaptic cell type (either corticotectal, corticostriatal or corticocortical) was multiplied by each dendritic length density map of each cell of the relevant postsynaptic cell type. Because the pairs of cells we studied were separated by an average of $53 \pm 24 \mu\text{m}$ (mean \pm s.d.; $n = 235$ pairs; range, 10–200 μm), we shifted the dendritic length density map 50 μm relative to the axonal length density map to estimate the spatial overlap. These results are compared with the measured physiological connectivity (Fig. 3). Because the distance between pairs of recorded cells ranged from 10 to 200 μm , we also shifted the dendritic length density maps from 0 to 200 μm relative to the axonal length density maps. We performed similar analyses with the neurons aligned by their soma position. Also, we restricted the analysis to the perisomatic dendritic processes, as this is where synapses among L5 pyramidal neurons are largely located^{10,11,15,26}. These manipulations all resulted in axodendritic overlaps similar to those shown in Fig. 3 (data not shown).

Full Methods and any associated references are available in the online version of the paper at www.nature.com/nature.

Received 2 September; accepted 17 November 2008.

Published online 18 January 2009.

1. Jones, E. G. in *Cerebral Cortex* (eds Peters, A. & Jones, E. G.) 521–553 (Plenum, 1984).
2. Kisvarday, Z. F. *et al.* Synaptic targets of HRP-filled layer III pyramidal cells in the cat striate cortex. *Exp. Brain Res.* **64**, 541–552 (1986).
3. McGuire, B. A., Hornung, J. P., Gilbert, C. D. & Wiesel, T. N. Patterns of synaptic input to layer 4 of cat striate cortex. *J. Neurosci.* **4**, 3021–3033 (1984).
4. Braitenberg, V. & Schuz, A. *Cortex: Statistics and Geometry of Neuronal Connectivity* (Springer, 1998).
5. Kozloski, J., Hamzei-Sichani, F. & Yuste, R. Stereotyped position of local synaptic targets in neocortex. *Science* **293**, 868–872 (2001).
6. Song, S., Sjöström, P. J., Reigl, M., Nelson, S. & Chklovskii, D. B. Highly nonrandom features of synaptic connectivity in local cortical circuits. *PLoS Biol.* **3**, e68 (2005).
7. Wang, Y. *et al.* Heterogeneity in the pyramidal network of the medial prefrontal cortex. *Nature Neurosci.* **9**, 534–542 (2006).

8. Kampa, B. M., Letzkus, J. J. & Stuart, G. J. Cortical feed-forward networks for binding different streams of sensory information. *Nature Neurosci.* **9**, 1472–1473 (2006).
9. Yoshimura, Y., Dantzker, J. L. & Callaway, E. M. Excitatory cortical neurons form fine-scale functional networks. *Nature* **433**, 868–873 (2005).
10. Le Bé, J. V., Silberberg, G., Wang, Y. & Markram, H. Morphological, electrophysiological, and synaptic properties of corticocortical pyramidal cells in the neonatal rat neocortex. *Cereb. Cortex* **17**, 2204–2213 (2006).
11. Morishima, M. & Kawaguchi, Y. Recurrent connection patterns of corticostriatal pyramidal cells in frontal cortex. *J. Neurosci.* **26**, 4394–4405 (2006).
12. Kasper, E. M., Larkman, A. U., Lubke, J. & Blakemore, C. Pyramidal neurons in layer 5 of the rat visual cortex. I. Correlation among cell morphology, intrinsic electrophysiological properties, and axon targets. *J. Comp. Neurol.* **339**, 459–474 (1994).
13. Wang, Z. & McCormick, D. A. Control of firing mode of corticotectal and corticopontine layer V burst-generating neurons by norepinephrine, acetylcholine, and 15,3R-ACPD. *J. Neurosci.* **13**, 2199–2216 (1993).
14. Hattox, A. M. & Nelson, S. B. Layer V neurons in mouse cortex projecting to different targets have distinct physiological properties. *J. Neurophysiol.* **98**, 3330–3340 (2007).
15. Markram, H., Lubke, J., Frotscher, M., Roth, A. & Sakmann, B. Physiology and anatomy of synaptic connections between thick tufted pyramidal neurones in the developing rat neocortex. *J. Physiol. (Lond.)* **500**, 409–440 (1997).
16. Thomson, A. M., Deuchars, J. & West, D. C. Large, deep layer pyramid-pyramid single axon EPSPs in slices of rat motor cortex display paired pulse and frequency-dependent depression, mediated presynaptically and self-facilitation, mediated postsynaptically. *J. Neurophysiol.* **70**, 2354–2369 (1993).
17. Mercer, A. *et al.* Excitatory connections made by presynaptic cortico-cortical pyramidal cells in layer 6 of the neocortex. *Cereb. Cortex* **15**, 1485–1496 (2005).
18. Hellwig, B. A quantitative analysis of the local connectivity between pyramidal neurons in layers 2/3 of the rat visual cortex. *Biol. Cybern.* **82**, 111–121 (2000).
19. Binzegger, T., Douglas, R. J. & Martin, K. A. A quantitative map of the circuit of cat primary visual cortex. *J. Neurosci.* **24**, 8441–8453 (2004).
20. Stepanyants, A. & Chklovskii, D. B. Neurogeometry and potential synaptic connectivity. *Trends Neurosci.* **28**, 387–394 (2005).
21. Kalisman, N., Silberberg, G. & Markram, H. Deriving physical connectivity from neuronal morphology. *Biol. Cybern.* **88**, 210–218 (2003).
22. Hallman, L. E., Schofield, B. R. & Lin, C. S. Dendritic morphology and axon collaterals of corticotectal, corticopontine, and callosal neurons in layer V of primary visual cortex of the hooded rat. *J. Comp. Neurol.* **272**, 149–160 (1988).
23. Hubener, M. & Bolz, J. Morphology of identified projection neurons in layer 5 of rat visual cortex. *Neurosci. Lett.* **94**, 76–81 (1988).
24. Larsen, D. D., Wickersham, I. R. & Callaway, E. M. Retrograde tracing with recombinant rabies virus reveals correlations between projection targets and dendritic architecture in layer 5 of mouse barrel cortex. *Front. Neural Circuits*. doi:10.3389/neuro.04.005.2007 (2008).
25. Shepherd, G. M., Stepanyants, A., Bureau, I., Chklovskii, D. & Svoboda, K. Geometric and functional organization of cortical circuits. *Nature Neurosci.* **8**, 782–790 (2005).
26. Frick, A., Feldmeyer, D., Helmstaedter, M. & Sakmann, B. Monosynaptic connections between pairs of L5A pyramidal neurons in columns of juvenile rat somatosensory cortex. *Cereb. Cortex* **18**, 397–406 (2008).
27. Stern, E. A., Jaeger, D. & Wilson, C. J. Membrane potential synchrony of simultaneously recorded striatal spiny neurons *in vivo*. *Nature* **394**, 475–478 (1998).
28. Douglas, R. J., Koch, C., Mahowald, M., Martin, K. A. & Suarez, H. H. Recurrent excitation in neocortical circuits. *Science* **269**, 981–985 (1995).
29. Swadlow, H. A. Efferent neurons and suspected interneurons in binocular visual cortex of the awake rabbit: receptive fields and binocular properties. *J. Neurophysiol.* **59**, 1162–1187 (1988).
30. Singer, W., Tretter, F. & Cynader, M. Organization of cat striate cortex: a correlation of receptive-field properties with afferent and efferent connections. *J. Neurophysiol.* **38**, 1080–1098 (1975).

Supplementary Information is linked to the online version of the paper at www.nature.com/nature.

Acknowledgements We thank J. Li and S. Pak for technical assistance. This work was supported by National Institutes of Health grants to S.P.B. and to S.H.

Author Contributions S.P.B. and S.H. designed the experiments. S.P.B. collected the data and S.P.B. and S.H. performed the analyses. S.P.B. and S.H. wrote the paper.

Author Information Reprints and permissions information is available at www.nature.com/reprints. Correspondence and requests for materials should be addressed to S.H. (shaul.hestrin@stanford.edu).

METHODS

Neuronal labelling. All experimental procedures were approved by the Institutional Animal Care and Use Committee of Stanford University. Juvenile mice (P14 to P17; C57BL/6 x CD-1 and YFP H-line³¹), were anaesthetized and placed in a stereotaxic frame. Using stereotaxic coordinates adjusted for the age of the mice³², two to 15 sites in the striatum, the superior colliculus and/or the contralateral cortex were injected with 50 nl of a suspension of fluorescently labelled latex microspheres³³ (red or green RetroBeads, Lumafuor). Buprenorphine (0.05 mg kg⁻¹) was administered to alleviate post-operative discomfort. Injections into the superior colliculus labelled neurons in L5 of the ipsilateral visual cortex. Injections into the striatum labelled neurons in layers 2/3 and 5 of ipsilateral and contralateral cortices. Only those cells in L5 of the cortex contralateral to the injection site, representing a subset of corticostriatal cells whose projections include the contralateral striatum, were targeted for further study^{34–36}. When studying corticocortical connections, we always simultaneously labelled corticocortical and corticotectal neurons by injecting beads of one colour into the contralateral visual cortex and beads of the other colour in the ipsilateral superior colliculus. There was essentially no overlap between these two cell populations^{22,23}. Only those corticocortical cells that intermingled with retrogradely labelled corticotectal pyramidal neurons in L5 were targeted for physiological study. To verify the stereotaxic coordinates of the injections, injected hemispheres were fixed, sectioned and mounted for visualization (Vectashield, Vector Laboratories).

Slice preparation and cell identification. One or more days after the injections, each mouse was anaesthetized and decapitated in an ice-cold sucrose solution composed of 75 mM sucrose, 76 mM NaCl, 25 mM NaHCO₃, 25 mM glucose, 2.5 mM KCl, 1.25 mM NaH₂PO₄, 7 mM MgCl₂, 0.5 mM CaCl₂, pH 7.4, 325 mosM. Parasagittal cortical slices, 300-µm thick, were sectioned from the selected hemisphere glued on a ramp set at a 30° angle (Integralslice 7550 MM, Campden Instruments), and were maintained in the same solution at 32–34 °C for 30 min before being transferred to artificial cerebrospinal fluid composed of 125 mM NaCl, 2.5 mM KCl, 1.25 mM NaH₂PO₄, 1 mM MgSO₄, 2 mM CaCl₂, 26 mM NaHCO₃, 20 mM glucose, 4 mM lactic acid, 2 mM pyruvic acid and 0.4 mM ascorbic acid, pH 7.4, 325 mosM, at room temperature (22–25 °C). All solutions were continuously bubbled with 95% O₂ and 5% CO₂. Retrogradely labelled neurons were identified under epifluorescent illumination (Axioskop 2 FS Plus, ×40 objective, numerical aperture 0.8, Zeiss) and targeted for recording using infrared differential-interference-contrast video microscopy (Sensicam QE, Cooke Corporation).

Electrophysiological recordings. Glass electrodes (2–4 mΩ) were filled with an internal solution containing 2.7 mM KCl, 120 mM potassium methylsulfate, 9 mM HEPES, 0.18 mM EGTA, 4 mM MgATP, 0.3 mM NaGTP, 20 mM phosphocreatine(Na), pH 7.3, 295 mosM. Simultaneous whole-cell patch clamp recordings of the targeted pyramidal cells were obtained using two Multiclamp 700A patch amplifiers (Molecular Devices) in current-clamp mode. All experiments were performed at 32–35 °C. Results were not corrected for the liquid junction potential.

Data acquisition and analysis. All data acquisition and analysis was performed using custom software written in IGOR Pro (Wavemetrics) or Matlab (Mathworks). To compare the adaptation rate of the three cell types, we injected a 200-ms step of depolarizing current adjusted to elicit six to 13 action potentials. A line was fitted to the plot of interspike intervals (ISIs) for each cell (Supplementary Fig. 1d). The first two ISIs were omitted from the analysis because corticotectal cells fired a burst at the start of the current injection. The slope was then divided by the mean ISI to generate an adaptation index for each cell. An adaptation index of zero indicates no adaptation in the spike rate. A positive adaptation index indicates an adapting spike train, whereas a negative adaptation index indicates a spike train with increasingly shorter ISIs. The sag was assessed by fitting a single exponential to the recovery from a hyperpolarizing current step.

Synaptic connectivity was typically assessed by averaging 25 or more traces with two presynaptic action potentials at 20 or 25 Hz and/or 12 presynaptic action potentials at 100 Hz. Each presynaptic action potential was generated

by a 3-ms injection of current, and individual trials were separated by 10 s. The 555 potential connections were classified as connected or unconnected while blinded to the identity of the presynaptic and postsynaptic neurons. Recorded neurons were separated by less than 200 µm (mean distance, 53 ± 24 µm (mean ± s.d.); $n = 235$ pairs). There was no significant difference in the distance between pairs of connected neurons and pairs of unconnected neurons for all connection types tested (data not shown). A bias in the vertical position of corticocortical and corticotectal neurons could not account for the differences in connectivity observed. The vertical distance we measured was a positive number when the corticocortical cell was above the corticotectal cell and was negative when the corticocortical cell was below the corticotectal cell. The mean vertical distance was 1 ± 33 µm (mean ± s.d.), which is not significantly different from zero ($P = 0.83$, $n = 86$). There was also no difference in the vertical arrangement of connected and unconnected corticocortical-to-corticotectal pairs ($P = 0.51$).

Morphologic reconstruction and analysis. To reveal the morphology of the recorded neurons, 0.25% w/v biocytin was included in the pipette recording solution of at least one of the pipettes. Following the physiological recordings, the tissue was processed using standard techniques to visualize the neurons with diaminobenzidine. The axons and dendrites of well-stained neurons were reconstructed in three dimensions using a NeuroLucida system (Microbrightfield) and a ×100 oil-immersion objective (numerical aperture 1.4, Zeiss). No correction was made for tissue shrinkage.

To analyse the distribution of neuronal processes for each cell, we measured the total length of dendrite or axon for each 50 µm × 50 µm × 300 µm cuboid in a 60 × 40 grid using Neuroexplorer (Microbrightfield). All reconstructed processes were included in this volume. Results from individual cells were then aligned either by soma position or relative to the pial margin. To estimate the spatial overlap of the dendritic and axonal processes of corticotectal, corticostriatal and corticocortical pyramidal neurons, we multiplied each axonal length density map by each dendritic length density map for each combination of cell types tested physiologically, to generate an estimate of the potential number of synapses formed between a pair of neurons. The results were used to compare the potential synaptic connectivity for each combination of cell pairs.

Results are expressed as means plus standard errors unless otherwise noted. The physiological and morphological properties of the three cell types were compared using one-way analysis of variance or the Kruskal–Wallis analysis of variance for multiple comparisons. When only two cell types were compared, Student's *t*-test was used. The probability of connection was assessed using Pearson's chi-squared test (two tailed). The relationship between the connectivity and the axodendritic overlap was also assessed, using a bootstrap approach to test the null hypothesis that the connectivity and the dendritic overlap were linearly related with a slope of one. The *P* values ranged from 0.017 to 0.039 using this approach for all the different configurations tested. These configurations included aligning the cell pairs relative to the pial margin or the cell bodies, separating the cell pairs by up to 200 µm, the largest separation in our physiological data set, and including only the perisomatic dendrites in the analysis.

31. Feng, G. *et al.* Imaging neuronal subsets in transgenic mice expressing multiple spectral variants of GFP. *Neuron* **28**, 41–51 (2000).
32. Paxinos, G. & Franklin, K. B. J. *The Mouse Brain in Stereotaxic Coordinates* (Academic, 2001).
33. Katz, L. C., Burkhalter, A. & Dreyer, W. J. Fluorescent latex microspheres as a retrograde neuronal marker for in vivo and in vitro studies of visual cortex. *Nature* **310**, 498–500 (1984).
34. Wilson, C. J. Morphology and synaptic connections of crossed corticostriatal neurons in the rat. *J. Comp. Neurol.* **263**, 567–580 (1987).
35. Lei, W., Jiao, Y., Del Mar, N. & Reiner, A. Evidence for differential cortical input to direct pathway versus indirect pathway striatal projection neurons in rats. *J. Neurosci.* **24**, 8289–8299 (2004).
36. Reiner, A., Jiao, Y., Del Mar, N., Laverghetta, A. V. & Lei, W. L. Differential morphology of pyramidal tract-type and intratelencephalically projecting-type corticostriatal neurons and their intrastriatal terminals in rats. *J. Comp. Neurol.* **457**, 420–440 (2003).